AIAA SciTech Forum
6-10 January 2020, Orlando, FL
AIAA Scitech 2020 Forum

10.2514/6.2020-1146

Semi-Intrusive Uncertainty Propagation and Adjoint Sensitivity Analysis Using the Stochastic Galerkin Method

Komahan Boopathy* and Graeme J. Kennedy†
Georgia Institute of Technology, Atlanta, GA, 30332-0150, USA.

Stochastic Galerkin projection techniques provide an efficient method to propagate uncertainties through simulations governed by differential equations. However, stochastic Galerkin methods are often challenging to implement within existing deterministic finite-element libraries and may require extensive source code modifications. In this work, we present a semi-intrusive stochastic Galerkin methodology that fully reuses existing deterministic finite-element implementations to perform projection in the probabilistic domain. Furthermore, the proposed semi-intrusive technique enables the use of deterministic derivatives for the adjoint method, yielding a stochastic Galerkin adjoint without further implementation effort. The principal idea is to project the deterministic element residuals, Jacobians, boundary conditions, and adjoint terms on to the probabilistic space prior to assembly of the stochastic finite element system, assuming the deterministic implementations to be black-box. The deterministic implementations must support the ability to update random parameters to enable quadrature in the stochastic space. The proposed semi-intrusive stochastic Galerkin approach is demonstrated using TACS, a finite-element framework with a adjoint-based gradient evaluation methods. The capabilities are demonstrated on several test problems including a flexible multibody dynamics simulation of a four bar mechanism.

Nomenclature

$x, \mathcal{X}$	spatial variable and domain
$t, \mathcal{T}$	temporal variable and domain
$y, \mathcal{Y}$	generalized probabilistic random variable and domain
$z, \mathcal{Z}$	standardized probabilistic random variable and domain
$\xi, \mathcal{D}$	design variable and domain
$u(t,y)$, $\dot{u}(t,y)$, $\ddot{u}(t,y)$	field/state variables and their time derivatives after spatial discretization
R	governing equations of probabilistic-spatio-temporal physics
$F(\xi,\cdot)$	metric of interest/objective functions
$G(\xi,\cdot)$	inequality constraint functions
$H(\xi,\cdot)$	equality constraint functions
$\mathbb{E}[F(y(\xi),\cdot)]$	expectation operator
$\mathbb{V}[F(y(\xi),\cdot)]$	variance operator
$\mathbb{S}[F(y(\xi),\cdot)]$	standard deviation operator

I. Introduction

Optimization under uncertainty (OUU) [1–8] has evolved as a field to account for the effect of uncertainties in an optimal design process. A key aspect of OUU is the propagation of uncertainty from random input parameters, through nonlinear numerical simulations, to obtain the expectation and variance of functions of interest. Various methods have been proposed for uncertainty propagation which tradeoff computational cost and implementation difficulty. Often, these methods are divided into either non-intrusive sampling-based methods or intrusive projection-based methods. Sampling-based methods are simple to use since they treat the deterministic code as a black-box. However these methods may be slow to converge, requiring many simulations. On the other hand, projection-based methods require explicit source code modification to perform integration in probabilistic space, but can provide more accuracy at less

*Graduate Student, School of Aerospace Engineering, 270 Ferst Drive, komahan@gatech.edu, AIAA Student Member.
†Assistant Professor, School of Aerospace Engineering, 270 Ferst Drive, graeme.kennedy@aerospace.gatech.edu, AIAA Senior Member.

computational cost. The application of projection-based methods, however, is limited due to the extra effort involved in code development [9].

In this work, we present a semi-intrusive approach to bridge this gap and take a step in furthering the applicability of projection-based methods in a more general stochastic finite-element setting. To demonstrate this approach, we extend a deterministic finite element analysis process to a stochastic finite element analysis process by reusing existing deterministic finite element capabilities. As Krenk and Gutirez [3] identify, projection-based methods for problems involving nonlinearities have not yet reached a mature stage. Xiu [9] also acknowledges the difficulty in deriving explicit stochastic nonlinear equations for nonlinear physical models. As a remedy to this problem, we propose an implicit formulation of stochastic algebraic equations, which circumvents the need for explicit stochastic equations. We apply this semi-intrusive framework to time-dependent simulations of flexible multibody dynamic systems. The use of time domain simulations poses the additional difficulty of integrating stochastic differential equations in time. This challenge is addressed by extending deterministic time-integration methods to the stochastic problem. To perform efficient gradient-based optimization, we develop an adjoint method for the projection-based simulation that leverages the deterministic implementation. The development of efficient adjoint methods is time consuming, however the proposed framework utilizes the deterministic implementation for the most challenging components of the adjoint method. The uncertainty framework is illustrated in Figure 1 which shows the integration of time-dependent physics, uncertainty analysis, and gradient evaluation using the adjoint method.

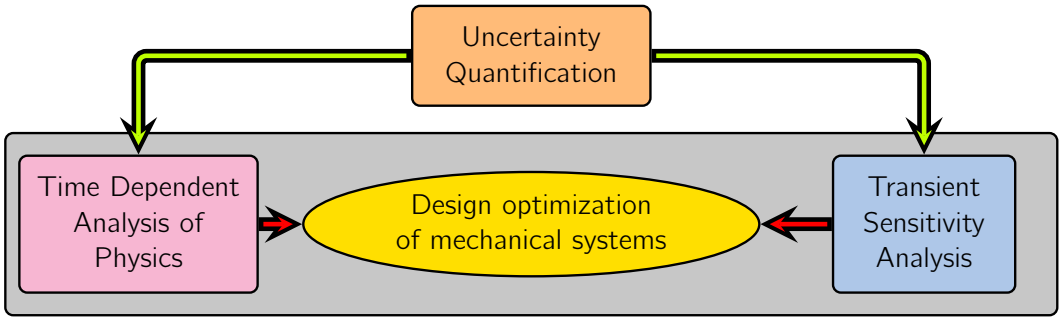

Figure 1: An integrated design framework with time-dependent physics, uncertainty quantification and adjoint-based gradient evaluation.

II. Design in the Presence of Probabilistically Modeled Uncertainties

Designing systems in the presence of uncertainties is composed of two main phases: uncertainty quantification and optimization under uncertainty. The uncertainty quantification (UQ) phase deals with the mathematical aspects of the uncertainty analysis, whereas the OUU phase deals with the mathematical aspects of formulating design requirements as objective or constraint functions.

A. Stages in Uncertainty Quantification

The UQ process is broken down in to three stages as:

1. Characterizing the source and form of uncertainties as mathematical functions (e.g. distribution types, intervals);
2. Propagating the input uncertainties through mathematical models of mechanical systems; and
3. Characterizing the behavior of output functions of interest.

The schematic of the UQ process is shown in Figure 2 and reviewed in the remainder of this section.

1. Stage I: Characterization of Input Uncertainties

In the setting of partial differential equations, uncertainties can be a part of input functions, that collectively refer to the functions describing the distribution of coefficients and physical properties (e.g. material properties, viscosity), forcing functions (e.g. lift distribution on wing, controller input), and initial as well as boundary conditions. These uncertainties can be characterized probabilistically using probability theory, or nonprobabilistically without probability theory.

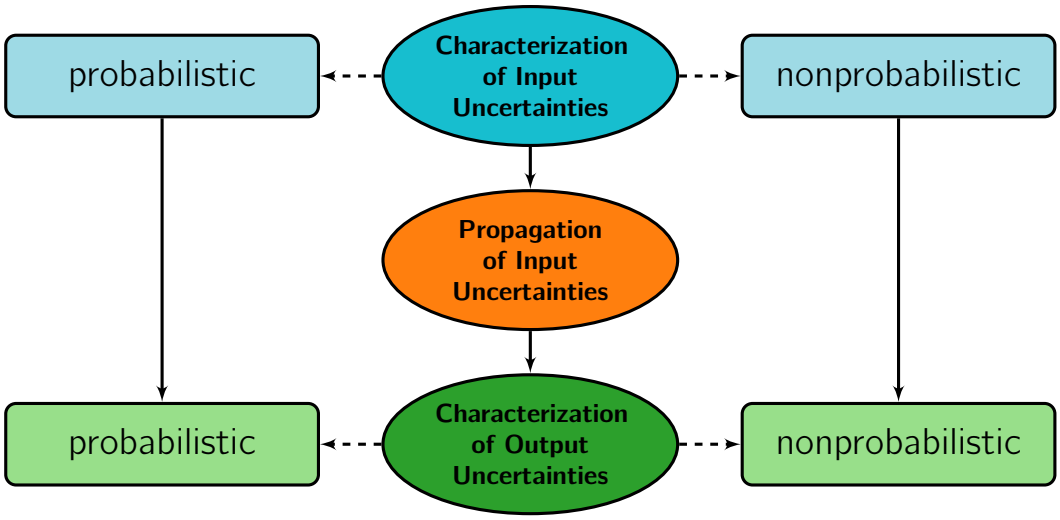

Figure 2: The three stages in uncertainty quantification.

(1) PROBABILISTIC CHARACTERIZATION (ALEATORY VARIABLES): When deterministic specification of these input functions become difficult due to the lack of sufficient information, then probabilistic specification in the form of probability density functions (PDFs) can be beneficial. For example, instead of specifying one value for a representative force acting on a mechanical structure, the probability distribution function of force could be a more relevant model of the real scenario. When the input functions are probabilistically specified, the partial differential equations (PDEs) that operate on these input functions naturally inherit a probabilistic domain, $\mathcal{Y}$, along with the original spatial domain, $\mathcal{X}$, and temporal domain, $\mathcal{T}$. The variables from the probabilistic domain are referred to as random variables, analogous to spatial and temporal variables from respective domains. These random variables can arise naturally in the direct specification of PDE coefficients as random variables, or indirectly from the spatial and temporal discretization of correlated and uncorrelated random fields. Both sources are special cases of the general scenario where a vector of random variables are present in the problem (see Gunzburger [8]). Since the input functions contain an additional probabilistic domain, the deterministic PDEs that operate on these inputs, as well as the output functions of interest, acquire the probabilistic domain and become stochastic partial differential equations (SPDEs). This naturally gives rise to the need for development of numerical methods for partial differential equations with random input functions. It is worth noting that SPDEs contain derivatives only in spatial and temporal variables; there are no derivatives in terms of random variables. Thus, from a vector-space point of view, we only need to find a set of basis functions to span the probabilistic space, where we can decompose probabilistic processes. This is identical in principle to finding finite-element basis functions to represent spatial distribution of solution in spatial domain.

(2) NONPROBABILISTIC CHARACTERIZATION (EPISTEMIC VARIABLES): Sometimes, it is difficult to associate probability information with random variables due to lack of sufficient data. This happens because a large amount of empirical data is necessary to predict the distribution in first place. When data is not available, nonprobabilistic approaches such as possibility theory, interval analysis, convex modeling and evidence theory (see Keane and Nair [10]) are used. In this work, we assume that only probabilistically modeled uncertainties are a part of the physical model (see Boopathy and Rumpfkeil [11], Boopathy et al. [12] for a combined treatment of aleatory and epistemic variables).

2. *Stage II: Propagation of Input Uncertainties*

Uncertainty propagation is the second and step in uncertainty analysis. It can be performed using non-intrusive sampling-based or intrusive projection-based methods.

(1) STOCHASTIC SAMPLING METHODS: The first class of techniques for uncertainty propagation are based on the idea of sampling. Sampling based techniques, collectively referred to as stochastic sampling methods (SSMs) rely on repeated solutions of the deterministic PDE at specified values of uncertain parameters from the probabilistic domain. Since this approach does not mandate any changes to the existing source code of the PDE solver, sampling-based techniques are referred to as non-intrusive [13–15]. The most-widely known sampling based technique for uncertainty

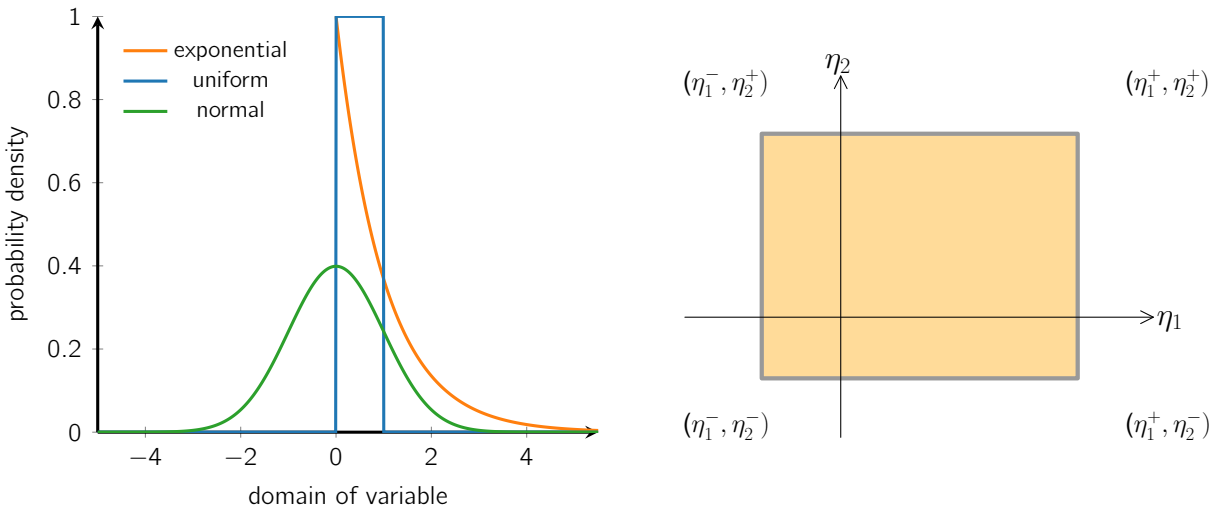

Figure 3: Probabilistic and non probabilistic modeling of uncertainties.

propagation is the Monte Carlo (MC) sampling [16, 17]. The MC method draws samples at random and it is the only method that does not suffer from the curse of dimensionality (the convergence is independent of the number of random variables), but the rate of convergence is rather limited to $\mathcal{O}(1/\sqrt{M})$, where M is the number of samples. A better selection of samples is offered by quasi-MC sampling methods (e.g. latin hypercube sampling), but at the cost of incurring a dependence on the number of variables and thus prone to the curse of dimensionality. The other type, namely, the quadrature sampling (also referred to as stochastic collocation) [18, 19], exploits the idea of Gaussian quadrature rules in the selection of sample points. This idea relies on the smoothness of interpolating polynomials and thus may not be suitable for functions with discontinuities. More restricting is the extension of one-dimensional quadrature rule to multiple dimensions using tensor product or similar rules, which leads to a very large number of points. In order to reduce the number of quadrature points, sparse quadrature methods have been proposed [8, 9, 20]. Since the reduction in number of quadrature points is achieved by exploiting the smoothness properties of solution, these methods are not suitable for non-smooth processes. Another approach is to build surrogate models [11, 12, 21–25] that are trained using a limited set of points (random, quasi-random or quadrature) and then replacing expensive deterministic solutions of PDE with inexpensive evaluations of the surrogate model. Sometimes the gradient information is also used in the construction of surrogate models alleviating the curse of dimensionality to an extent [23]. These SSMs allow great flexibility in using deterministic codes as black-box solvers, but accuracy, robustness, speed and efficiency are seldom found together in any of these methods. Figure 4 shows random, quasirandom and quadrature selection of samples from a two-dimensional random space.

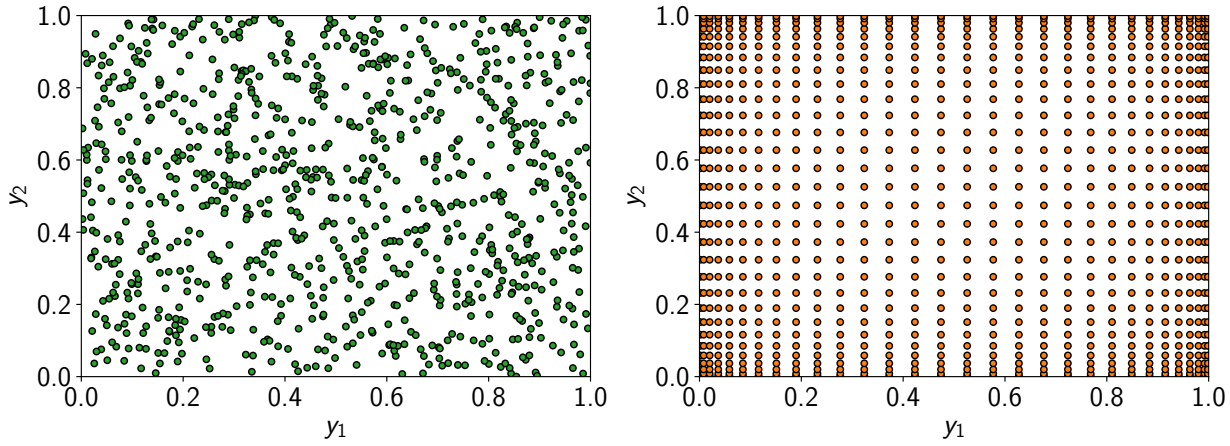

Figure 4: Selection of samples using random and quadrature sampling methods to evaluate multidimensional integrals.

(2) STOCHASTIC GALERKIN METHODS: The second class of techniques for uncertainty propagation are based on the idea of Galerkin projection in probabilistic space and are collectively referred to as stochastic Galerkin methods (SGMs) [5, 26, 27]. The SGMs differ from SSMs in that they directly solve the SPDEs to obtain the solution instead of solving the deterministic PDE multiple times. The SGM is amenable for the development of specialized algorithms aiming to exploit the nature of equations in stochastic solvers that perform computations in an efficient manner. However, this development requires significant effort in terms of specialized solvers, thus leading to its classification as intrusive methods [9].

Based on the construction of approximation to probabilistic space, SGMs can be further classified into a few subcategories. The use of globally orthonormal polynomials for the approximation of probabilistic space has led to the development of methods based on spectral expansion [9, 28], where the entries in basis set have global support. Since the basis functions have global support the spectral expansion type methods are not the ideal choice if there exists discontinuities of the solution in terms of probabilistic parameter space. This motivates the use of basis functions with local support, similar to localized finite-element type constructions that can treat discontinuities. Based on the spatial discretization method some approaches are referred to as stochastic finite element method [1–3, 29–31] and stochastic finite volume methods [32]. The methods used to effect spatial or temporal discretization is not as important as accurate and efficient stochastic projection to obtain the set of stochastic algebraic equations. Xiu *et al.*[9] points out that SGMs offer the most accurate solution possible with the least number of equations to be solved in the presence of large number of random variables, despite the coupling between probabilistic and physical degrees of freedom.

Although projecting in stochastic space appears to be a simple guiding principle, its implementation can be challenging. This has inhibited the wider adoption of SGMs, despite their potential benefits [9]. As Krenk and Gutirez [3] note, projection-based methods for problems involving nonlinearities have not yet reached a mature stage. When the governing deterministic PDEs take complex nonlinear coupled forms, the explicit derivation of stochastic equations (in algebraic form) may not be possible as noted by Xiu *et al.* [9]. This work considers this a motivation and intends to present the concept of projecting in stochastic space to get nonlinear stochastic algebraic equations with little to no reference to the physical context and spatial and temporal discretizations. We acknowledge the difficulty in obtaining nonlinear stochastic algebraic equations, and also point out that in reality, the explicit equations are not necessary and can be made an implicit part of computational machinery seeking the solution to SPDEs. As an analogy, it is sufficient if one is able to form Jacobian-vector products implicitly to be able to solve a linear system. We observe and emphasize that the stochastic residuals and Jacobians can be assembled on the fly as we compute and thus deriving explicit stochastic algebraic equations are not a necessity. It is sufficient to have deterministic algebraic equations resulting from the spatial discretization method of choice (finite element or finite volume). In this work we try to show the applicability of this guiding principle by demonstrating on problems ranging in complexities in a finite element setting.

3. *Stage III : Characterization of Output Uncertainties*

The final step of characterization of output uncertainties follow after the propagation of input uncertainties through the system models and the evaluation of metrics of interest. This stage is dependent on the first stage of uncertainty quantification; if nonprobabilistic methods are used to represent input uncertainties, then only nonprobabilistic information can be used to describe the behavior of outputs of the system. For example, when nonprobabilistic input bounds are processed into the analysis model, only bounds on the output metrics of interest can be constructed. Similarly, when inputs are probabilistically modeled, then probability distribution of the outputs can be obtained, along with useful probabilistic moments such as mean, variance and standard deviation. This output information can be used to formulate optimization under uncertainty problems.

B. Optimization Under Uncertainty

Within the OUU literature problems are typically classified as robustness-based formulations [33–50] or reliability-based formulations [51–53]. In this section, first we introduce a general optimization problem without the inclusion of uncertainties and later compare it to the problem statement where probabilistically modeled uncertainties are included A deterministic optimization problem can be written as

$$\begin{aligned} \underset{\xi}{\text{minimize}} \quad & F(\xi,\cdot) \\ \text{subject to} \quad & G(\xi,\cdot) \leq 0 \\ & H(\xi,\cdot) = 0 \end{aligned} \tag{1}$$

where ξ are the uncertain design variables, $F(\xi,\cdot)$ is the objective function, $G(\xi,\cdot)$ are the inequality constraint functions and $H(\xi,\cdot)$ are the equality constraint functions. The derivatives of the objective and constraint functions with respect to the design variables are required to solve the design problem (1) using gradient-based optimization.

1. *Probabilistic Optimization Under Uncertainty Formulation*

Historically, OUU problems have evolved separately as robust or reliable formulations. However, when designing systems in the presence of uncertainties, the designer is concerned about both robustness and reliability aspects of the design. For instance, the airplane should be designed to ensure fuel efficiency amidst of uncertain wind gusts (robustness) without compromising on the safety aspects (reliability). We find that robustness discussions arise on the side of objective function whereas reliability discussions arise on the side of constraints.

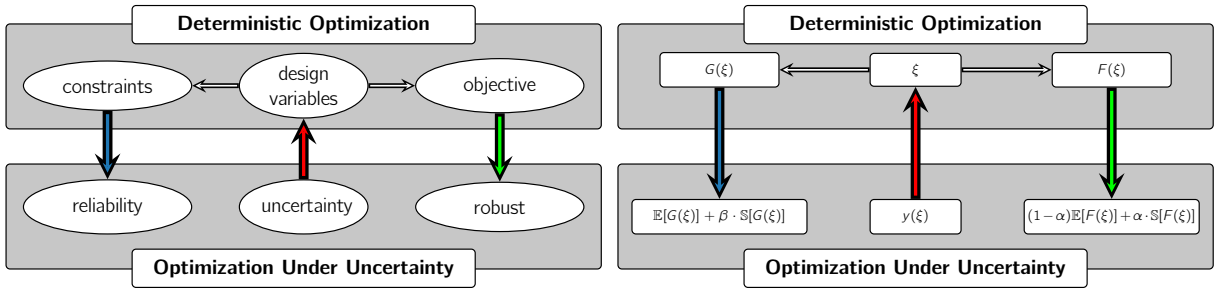

Figure 5: Origination of robustness and reliability arguments from the space of deterministic optimization as soon as uncertainties are introduced.

Figure 5 illustrates this idea along with mathematical statements that effect them. These mathematical statements are applicable only for probabilistically modeled uncertainties, whereas non-probabilistic models have different mathematical statements. The probabilistic moments such as the mean $\mathbb{E}[F(y(\xi),\cdot)]$, variance $\mathbb{V}[F(y(\xi),\cdot)]$, standard deviation $\mathbb{S}[F(y(\xi),\cdot)]$ and probability $\mathbb{P}[G(y(\xi),\cdot)\leq 0]$ need to be evaluated to formulate a probabilistic OUU problem.

DESIGN VARIABLES: The design variable vector ξ can contain deterministic variables and random variables. For the deterministic variables, there is no ambiguity in their selection since they simply refer to one value. In principle, the realizations of random variables can not be directly subject to design as they can take an infinite number of values. However, their probabilistic moments, such as the mean, may be included in the design problem. The design vector can therefore be written as

$$\vec{\xi} = [\ \underbrace{\xi_1,\xi_2,}_{\text{deterministic}}\ \underbrace{,y_1(\mu_{\xi_3}),y_2(\mu_{\xi_4})]}_{\text{random}} \tag{2}$$

OBJECTIVE FUNCTION: The objective of minimizing the expected performance and its variability can be stated mathematically as

$$\underset{\xi}{\text{minimize}} \quad \underbrace{(1-\alpha)\cdot\mathbb{E}[F(\xi,\cdot)]}_{\text{expected performance}} + \underbrace{\alpha\cdot\mathbb{S}[F(\xi,\cdot)]}_{\text{performance variability}} \tag{3}$$

with user-specified weights $\alpha\in[0,1]$ that can be interpreted as a tunable parameter controlling robustness. Equation (3) can be viewed as a multiobjective optimization problem or as augmenting the mean objective with a weighted penalization using standard deviation. Some authors use two unconstrained weights α_1 and α_2 as well as variance in place of standard deviation [24].

CONSTRAINT FUNCTION: The designer may want to enforce directly that the probability of inequality constraint violation is less than a small number, for instance as $\mathbb{P}[G(y(\xi),\cdot)\leq 0]\geq b\%$. The probabilistic moments such as mean, variance and standard deviations are computationally easier to evaluate compared to the direct evaluation of probabilities. Therefore, an explicit enforcement of probabilities are difficult, where one can use implicit moment matching formulations (see Parkinson et al. [54], Du and Chen [50], Du and Chen [55]) to achieve the same effect. The probability statement can be restated as

$$\mathbb{P}[G(y(\xi),\cdot)\leq 0]\geq b\% \longrightarrow \underbrace{\mathbb{E}[G(\xi,\cdot)]}_{\text{location of constraint manifold}} + \underbrace{\beta\cdot\mathbb{S}[G(\xi,\cdot)]}_{\text{shifting constraint manifold}} \leq 0 \tag{4}$$

where b is the desired probability and $\beta \in [0,\infty)$ can be interpreted as a tunable parameter controlling reliability. The enforcement of equality constraints is rather tricky; see Rangavajhala et al. [56] for an overview of treatment of equality constraints. The simplest method is ensuring that the the optimal solution is sought along the manifold pertaining to expectation of equality constraint as

$$\mathbb{E}[H(\xi,\cdot)] = 0. \tag{5}$$

PROBABILISTIC OUU PROBLEM STATEMENT: Therefore, a general OUU problem embedding optimality, robustness and reliability design considerations can be stated as

$$\begin{aligned} \underset{\xi}{\text{minimize}} \quad & (1-\alpha)\mathbb{E}[F(\xi,\cdot)] + \alpha \cdot \mathbb{S}[F(\xi,\cdot)] \\ \text{subject to} \quad & \mathbb{E}[G(\xi,\cdot)] + \beta \cdot \mathbb{S}[G(\xi,\cdot)] \leq 0 \\ & \mathbb{E}[H(\xi,\cdot)] = 0 \end{aligned} \tag{6}$$

The solution of the OUU problem (6) using gradient based optimization requires the derivatives

$$\frac{d\mathbb{E}[F(\xi,\cdot)]}{d\xi}, \frac{d\mathbb{E}[G(\xi,\cdot)]}{d\xi}, \frac{d\mathbb{E}[H(\xi,\cdot)]}{d\xi}, \frac{d\mathbb{S}[F(\xi,\cdot)]}{d\xi}, \frac{d\mathbb{S}[G(\xi,\cdot)]}{d\xi}.$$

The evaluation of these derivatives will be described below.

III. Uncertainty Propagation Through Physics and Sensitivity Analysis Equations

The spatial discretization of nonlinear PDEs results in a system of nonlinear ordinary differential equations (ODEs) in time, which are denoted as R. The solution of these nonlinear ODEs is then used for the evaluation of functions of interest, which are denoted as F. This process can be stated mathematically as:

$$\begin{aligned} \underset{u(t,\xi),\dot{u}(t,\xi),\ddot{u}(t,\xi)}{\text{solve}} \quad & R(t,\xi,u(t,\xi),\dot{u}(t,\xi),\ddot{u}(t,\xi)) = 0 \\ \text{evaluate} \quad & F(t,\xi,u(t,\xi),\dot{u}(t,\xi),\ddot{u}(t,\xi)). \end{aligned} \tag{7}$$

where $u(t,\xi)$ is the unknown function characterizing the physical state of the system, with the first and second time derivatives, $\dot{u}(t,\xi)$ and $\ddot{u}(t,\xi)$, respectively. Note that t is the temporal variable from time domain $\mathcal{T}$ and ξ is the design variable from design parameter domain $\mathcal{D}$. The solution of nonlinear ODEs is performed via implicit time integration techniques, where the nonlinear algebraic system at each time step is solved using a Newton–Raphson technique which requires the formation of residuals and Jacobian matrices. The full details of these time integration techniques and their corresponding adjoint implementation are described in Boopathy and Kennedy [57, 58].

With the inclusion of probabilistically modeled uncertainties, the deterministic ODEs become stochastic ODEs. The stochastic analysis problem can be stated mathematically as follows

$$\begin{aligned} \underset{u(t,y(\xi)),\dot{u}(t,y(\xi)),\ddot{u}(t,y(\xi))}{\text{solve}} \quad & R(t,y(\xi),u(t,y(\xi)),\dot{u}(t,y(\xi)),\ddot{u}(t,y(\xi))) = 0 \\ \text{evaluate} \quad & \mathbb{E}\left[F(t,y(\xi),u(t,y(\xi)),\dot{u}(t,y(\xi)),\ddot{u}(t,y(\xi)))\right] \\ & \mathbb{V}\left[F(t,y(\xi),u(t,y(\xi)),\dot{u}(t,y(\xi)),\ddot{u}(t,y(\xi)))\right] \\ & \mathbb{S}\left[F(t,y(\xi),u(t,y(\xi)),\dot{u}(t,y(\xi)),\ddot{u}(t,y(\xi)))\right] \end{aligned} \tag{8}$$

Once the unknown stochastic state fields $u(t,y(\xi))$, $\dot{u}(t,y(\xi))$ and $\ddot{u}(t,y(\xi))$ are determined, the probabilistic moments such as the mean $\mathbb{E}[F]$, variance $\mathbb{V}[F]$ and standard deviation $\mathbb{S}[F]$ can be evaluated.

A. Galerkin Projection Method

Given a set of initial *non-orthonormal* polynomials spanning the generalized probabilistic space $\mathcal{Y}$, we construct an *orthogonal* and *orthonormal* set of polynomial basis functions spanning the same space $\mathcal{Y}$ using Gram–Schmidt process such that

$$\mathcal{Y} = \underset{\textit{initial set}}{\text{span}}\{\psi_i(y)\}_{i=1}^{N} = \underset{\textit{orthogonal set}}{\text{span}}\{\overline{\psi}_i(y)\}_{i=1}^{N} = \underset{\textit{orthonormal set}}{\text{span}}\{\widehat{\psi}_i(y)\}_{i=1}^{N} \tag{9}$$

The orthonormality of any two basis functions $\widehat{\psi}_i(y)$ and $\widehat{\psi}_j(y)$ is mathematically defined as

$$\left\langle \widehat{\psi}_i(y) \;\middle|\; \widehat{\psi}_j(y) \right\rangle_{\rho(y)}^{\mathcal{Y}} = \int_{\mathcal{Y}} \widehat{\psi}_i(y)\rho(y)\widehat{\psi}_j(y)\, dy = \begin{cases} 1 & \text{if } i = j \\ 0 & \text{if } i \neq j \end{cases}, \tag{10}$$

where $\rho(y) \geq 0$ for $y \in \mathcal{Y}$ is the probability density function corresponding to the distribution type of the random variable y. The orthonormal polynomials for probability distribution types used in this work are listed in Table 1 for a standard probabilistic variable z from the standard probabilistic space $\mathcal{Z}$. Since, the orthonormal polynomial set is derived for standard probability distributions, transformation of variables must be used when performing inner products in the generalized probabilistic domain $\mathcal{Y}$. The standardization is usually done with zero location and unit stretch as distribution parameters.

Table 1: Orthonormal polynomials for standard probability distributions.

	Hermite	Legendre	Laguerre
distribution	$\mathcal{N}(y;\mu=0,\sigma=1)$	$\mathcal{U}(y;a=0,b=1)$	$\mathcal{E}(y;\mu=0,\beta=1)$
standardization	$z=\frac{y-\mu}{\sigma}$	$z=\frac{y-a}{b-a}$	$z=\frac{y-\mu}{\beta}$
notation	$\widehat{H}_d(z)$	$\widehat{P}_d(z)$	$\widehat{L}_d(z)$
weight	$\frac{1}{\sqrt{2\pi}}\exp\left(-\frac{1}{2}z^2\right)$	1	$\exp(-z)$
orthogonal set	$\overline{H}_d(z)$	$\overline{P}_d(z)$	$\overline{L}_d(z)$
0	1	1	1
1	z	$2z-1$	$-z+1$
$\vdots$	$\vdots$	$\vdots$	$\vdots$
d	$z\overline{H}^z_{d-1}(z)-(d-1)\overline{H}^z_{d-2}(z)$	$(-1)^d\sum_{k=0}^{d}\binom{d}{k}\binom{d+k}{k}(-z)^k$	$\frac{(2d-1-z)\,\overline{L}^z_{d-1}(z)}{d} - \frac{(d-1)\overline{L}^z_{d-2}(z)}{d}$
normalization	$\widehat{H}^z_d(z)=\overline{H}^z_d(z)/\sqrt{d!}$	$\widehat{P}^z_d(z)=\overline{P}^z_d(z)\sqrt{2d+1}$	$\widehat{L}^z_d(z)=\overline{L}^z_d(z)$

1. *Formation of Stochastic States*

We begin the solution process to (8) using the stochastic Galerkin method with the following hypothesis for stochastic state functions:

$$u(t,y) \approx \sum_{i=1}^{N} u_i(t)\,\widehat{\psi}_i(y) \tag{11}$$

This expansion can be interpreted as an application of the technique of separation of variables for solving differential equations. Due to global support nature of the basis functions $\widehat{\psi}(y)$, the equations (11) are referred to as a spectral expansion of probabilistic functions in orthonormal basis. Alternatively, $\widehat{\psi}(y)$ can be constructed so as to have compact support, resulting in a treatment similar to finite-element methodology.

2. *Formation of Stochastic Residual*

The stochastic residuals are formed by projecting deterministic residuals onto each basis function $\widehat{\psi}_i(y)$ in the basis set spanning the probabilistic space $\mathcal{Y}$

$$\left\langle \widehat{\psi}_i(y) \;\middle|\; R(t,y,u(t,y),\dot{u}(t,y),\ddot{u}(t,y)) \right\rangle_{\rho(y)}^{\mathcal{Y}} \approx R_i \triangleq \sum_{q=1}^{Q} \alpha_q \widehat{\psi}_i(y_q) \underbrace{R(t,y_q,u(t,y_q),\dot{u}(t,y_q),\ddot{u}(t,y_q))}_{\text{deterministic residual for } y_q} \tag{12}$$

We use numerical quadrature to approximate this inner product with Q quadrature points from probabilistic space $\mathcal{Y}$. The number of quadrature points necessary can sometimes be determined *a priori* using the polynomial degree of the

integrand. The full stochastic residual vector takes the form:

$$\mathcal{R} = \begin{bmatrix} R_1 \\ R_2 \\ \vdots \\ R_N \end{bmatrix} = \begin{bmatrix} \sum_{q=1}^{Q} \alpha_q \widehat{\psi_1}(y_q) R(t, y_q, u(t,y_q), \dot{u}(t,y_q), \ddot{u}(t,y_q)) \\ \sum_{q=1}^{Q} \alpha_q \widehat{\psi_2}(y_q) R(t, y_q, u(t,y_q), \dot{u}(t,y_q), \ddot{u}(t,y_q)) \\ \vdots \\ \sum_{q=1}^{Q} \alpha_q \widehat{\psi_N}(y_q) R(t, y_q, u(t,y_q), \dot{u}(t,y_q), \ddot{u}(t,y_q)) \end{bmatrix} \tag{13}$$

From (12) and (13), it is clear that the stochastic residual $\mathcal{R}$ can be computed using repeated evaluations of the deterministic residual R at quadrature points y_q.

3. *Formation of Stochastic Jacobian*

The stochastic Jacobian matrix can be computed using repeated evaluations of the deterministic Jacobian for each quadrature point. The block i, j entry of Jacobian is

$$\mathcal{J}_{i,j} \triangleq \frac{\partial R_i}{\partial u_j} = \sum_{q=1}^{Q} \alpha_q \widehat{\psi}_i(y_q) \widehat{\psi}_j(y_q) J(t, y_q, u(t,y_q), \dot{u}(t,y_q), \ddot{u}(t,y_q)), \tag{14}$$

where J is the deterministic Jacobian and Q is the number of quadrature points. As a result, the full stochastic Jacobian matrix takes the form

$$\mathcal{J} = \begin{bmatrix} \mathcal{J}_{1,1} & \mathcal{J}_{1,2} & \cdots & \mathcal{J}_{1,N} \\ \mathcal{J}_{21} & \mathcal{J}_{2,2} & \cdots & \mathcal{J}_{2,N} \\ \vdots & \vdots & \ddots & \vdots \\ \mathcal{J}_{N,1} & \mathcal{J}_{N,2} & \cdots & \mathcal{J}_{N,N} \end{bmatrix}. \tag{15}$$

Figure 6 illustrate the nonzero patterns of the Jacobian matrices for different stochastic basis choices. Notice that there are as many off-diagonal bands as the polynomial degree of the random variable. In this work we use full tensor product space for simplicity, although other constructions such as complete polynomials may be efficient. It is possible to determine the nonzero entries of the Jacobian *a priori*, if the polynomial degree of the random variables with in the system is known. Exploiting this sparsity can eliminate unnecessary computations in the assembly of stochastic Jacobians.

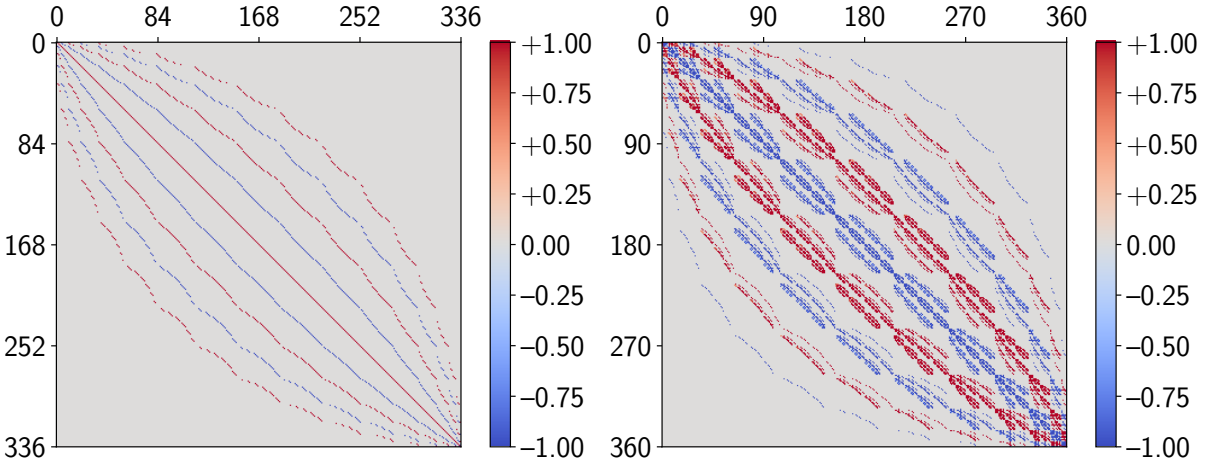

Figure 6: Sparsity patterns Jacobian matrices resulting from decomposition of for stateless Jacobian functions $J(y) = y_4^3$ (left) with $N = 336$ and $J(y) = y_1 y_2 y_3 y_4$ (right) with $N = 360$ in orthonormal space.

4. *Initial Conditions*

The projection of initial conditions and their time derivatives is performed as follows

$$\left\langle \widehat{\psi}_i(y) \,\middle|\, u(0,y) \right\rangle_{\rho(y)}^{\mathcal{Y}} \approx \sum_{q=1}^{Q} \alpha_q \widehat{\psi}_i(y_q) u(0, y_q) \tag{16}$$

This includes the case where the initial conditions also are dependent on random variables from probabilistic domain (uncertainty associated with initial conditions).

5. Formation of Stochastic Adjoint Equations

The stochastic adjoint states are the unknowns of the adjoint problem which takes the form

$$\mathcal{J}^T \lambda = \frac{\partial \mathcal{F}}{\partial \mathcal{U}}^T \tag{17}$$

The transpose stochastic Jacobian matrix can be computed in an analogous manner as the Jacobian matrix described above. The right hand side of the adjoint system of equations is formed by projecting the deterministic right hand side terms onto each basis entry in the orthonormal set as

$$\begin{bmatrix} \mathcal{J}_{1,1} & \mathcal{J}_{1,2} & \cdots & \mathcal{J}_{1,N} \\ \mathcal{J}_{21} & \mathcal{J}_{2,2} & \cdots & \mathcal{J}_{2,N} \\ \vdots & \vdots & \ddots & \vdots \\ \mathcal{J}_{N,1} & \mathcal{J}_{N,2} & \cdots & \mathcal{J}_{N,N} \end{bmatrix}^T \begin{bmatrix} \lambda_1 \\ \lambda_2 \\ \vdots \\ \lambda_N \end{bmatrix} = \frac{\partial \mathcal{F}}{\partial \mathcal{U}}^T \tag{18}$$

The solution of the stochastic state variables and their time derivatives allows the evaluation of probabilistic moments of quantities of interest. The solution of the stochastic adjoint variables allows the evaluation of the design variable derivatives of probabilistic moments.

6. Probabilistic Moments and Derivatives

The mathematical relations for the evaluation of probabilistic moments and its derivatives are derived first. Using the stochastic Galerkin expansion, the expectation of a function of interest $F(y,\cdot)$ is

$$\mathbb{E}[F(y,\cdot)] = \int_{\mathcal{Y}} \rho(y) F(y,\cdot)\, dy = \left\langle \widehat{\psi}_1(y) \;\middle|\; F(y,\cdot) \right\rangle_{\rho(y)}^{\mathcal{Y}} \approx \left\langle \widehat{\psi}_1(y) \;\middle|\; \sum_{i=1}^{N} F_i(\cdot)\widehat{\psi}_i(y) \right\rangle_{\rho(y)}^{\mathcal{Y}} = F_1(\cdot) \tag{19}$$

In a similar manner, the derivative of expectation of the function is obtained as

$$\mathbb{E}\left[\frac{dF(y,\cdot)}{d\xi}\right] = \frac{dF_1}{d\xi} \tag{20}$$

In the stochastic Galerkin method, the variance can be computed as

$$\mathbb{V}[F(y,\cdot)] = \mathbb{E}[F(y,\cdot)F(y,\cdot)] - \mathbb{E}[F(y,\cdot)]\mathbb{E}[F(y,\cdot)] \approx \sum_{i=2}^{N} F_i^2(\cdot) \tag{21}$$

Differentiating the above we get the derivative of variance as

$$\frac{d\mathbb{V}[F(y,\cdot)]}{d\xi} = 2\sum_{i=2}^{N} F_i(\cdot)\frac{dF_i}{d\xi} \tag{22}$$

The standard deviation of a function of interest can be obtained from the variance

$$\mathbb{S}[F(y,\cdot)] = \sqrt{\mathbb{V}[F(y,\cdot)}} \tag{23}$$

The derivative of standard deviation is

$$\frac{d\mathbb{S}[F(y,\cdot)]}{d\xi} = \frac{1}{2\sqrt{\mathbb{V}[F(y,\cdot)]}} \times \frac{d\mathbb{V}[F(y,\cdot)]}{d\xi} \tag{24}$$

These expressions will be used below to obtain estimates of the mean, variance and standard deviation and their derivatives with respect to the design variables.

B. Nonintrusive Sampling Method

The principle of nonintrusive methods is to repeatedly evaluate the function of interest at predetermined quadrature locations in the stochastic space, y_i, to compute the probabilistic moments and derivatives. The number of quadrature points M is chosen based on the accuracy required and the computational budget at hand. For nonintrusive sampling methods, the expectation of the function is approximated as

$$\mathbb{E}[F(y,\cdot)] = \underbrace{\int_{\mathcal{Y}} \rho(y) F(y,\cdot)\, dy}_{\text{integral}} \approx \underbrace{\sum_{i=1}^{M} \alpha_i F(y_i,\cdot)}_{\text{quadrature approximation}} \tag{25}$$

The derivative of expectation of function with respect to design variables ξ is

$$\frac{d\mathbb{E}[F(y,\cdot)]}{d\xi} = \frac{d}{d\xi}\left(\int_{\mathcal{Y}} \rho(y) F(y,\cdot)\, dy\right) \quad = \int_{\mathcal{Y}} \rho(y) \frac{dF(y,\cdot)}{d\xi}\, dy = \mathbb{E}\left[\frac{dF(y,\cdot)}{d\xi}\right] \tag{26}$$

The derivative of expectation of a function is identical to the expectation of the derivative of the same function. We approximate the derivative as

$$\frac{d\mathbb{E}[F(y,\cdot)]}{d\xi} \approx \sum_{i=1}^{M} \alpha_i \frac{dF(y_i,\cdot)}{d\xi} \tag{27}$$

For nonintrusive sampling methods, the variance of function can be obtained as

$$\begin{aligned} \mathbb{V}[F(y,\cdot)] &= \mathbb{E}[F(y,\cdot)F(y,\cdot)] - \mathbb{E}[F(y,\cdot)]\mathbb{E}[F(y,\cdot)] \\ &\approx \sum_{i=1}^{M} \alpha_i F^2(y_i,\cdot) - \left(\sum_{i=1}^{M} \alpha_i F(y_i,\cdot)\right)^2 \end{aligned} \tag{28}$$

The derivative of variance is

$$\begin{aligned} \frac{d\mathbb{V}[F(y,\cdot)]}{d\xi} &= \mathbb{E}\left[2F(y,\cdot)\frac{dF(y,\cdot)}{d\xi}\right] - 2\mathbb{E}[F(y,\cdot)]\frac{d\mathbb{E}[F(y,\cdot)]}{d\xi} \\ &\approx \left(2\sum_{i=1}^{M} \alpha_i F(y_i,\cdot)\frac{dF(y_i,\cdot)}{d\xi}\right) - 2\left(\sum_{i=1}^{M} \alpha_i F(y_i,\cdot)\right)\left(\sum_{i=1}^{M} \alpha_i \frac{dF(y_i,\cdot)}{d\xi}\right) \end{aligned} \tag{29}$$

IV. Results

In this section, we present the results of semi-intrusive uncertainty propagation and sensitivity analysis for time-dependent systems. We consider the following four test cases:

1. A first order ODE benchmark problem;
2. Pitching and plunging airfoil modeled using a second order ODE with two degrees of freedom;
3. Spring mass damper; and
4. Flexible four bar beam mechanism.

A. Uncertainty Analysis on Decay ODE

Consider the following first-order differential equation with prescribed initial condition u_0 and constant decay parameter λ

$$\begin{aligned} \frac{du(t)}{dt} + \lambda\, u(t) = 0 \quad &\in \quad \mathcal{T} \\ u(0) = u_0 \quad &\in \quad \partial\mathcal{T} \end{aligned} \tag{30}$$

The analytical solution to the differential equation is $u(t) = u_0\, \mathrm{e}^{-\lambda t}$. In this problem, the decay parameter is uncertain such that $\lambda := \lambda(y)$, where y is a random variable from stochastic domain $\mathcal{Y}$. This adds a stochastic dimension to the differential equation resulting in the stochastic differential equation

$$\begin{aligned} \frac{du(t,y)}{dt} + \lambda(y)\, u(t,y) = 0 \quad &\in \quad \mathcal{T}\otimes\mathcal{Y} \\ u(0,y) = u_0 \quad &\in \quad \partial\mathcal{T}\otimes\mathcal{Y} \end{aligned} \tag{31}$$

1. *Stochastic Quadrature Sampling (Normal Distribution)*

Stochastic sampling technique uses repeated solutions of the differential equation (31) to perform integration in the stochastic domain. The decay parameter value $\lambda_i = \lambda(y_i)$ depends on the random variable y_i and its corresponding distribution type. The stochastic ODE

$$\begin{aligned} \frac{du(t,y_i)}{dt} + \lambda_i u(t,y_i) = 0 \quad &\in \quad \mathcal{T} \otimes \mathcal{Y} \\ u(0,y_i) = u_0 \quad &\in \quad \partial\mathcal{T} \otimes \mathcal{Y} \end{aligned} \tag{32}$$

is solved for each $\lambda_i = \lambda(y_i)$ and the solutions $u(t,y_i)$ are stored. The moments of the solution are computed as

$$\begin{aligned} \mathbb{E}[u(t,y)] &= \sum_{i=1}^{M} \alpha_i u(t,y_i) \\ \mathbb{V}[u(t,y)] &= \sum_{i=1}^{M} \alpha_i u^2(t,y_i) - (\mathbb{E}[u(t,y)])^2 \end{aligned} \tag{33}$$

Figure 7 compares mean and variance computed using stochastic sampling method with analytical mean and variance for increasing number of samples from stochastic domain. It can be seen that the first moment converges faster than the second moment to the exact value.

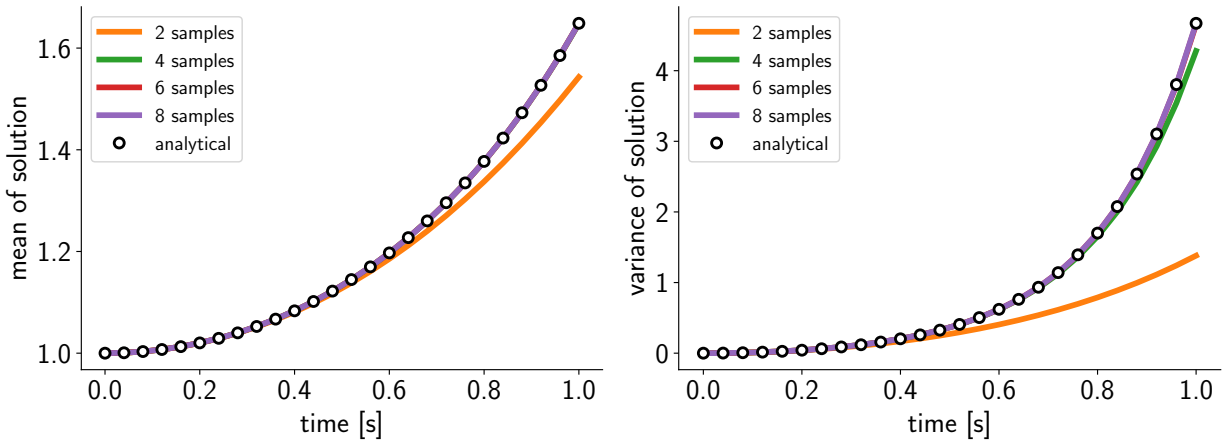

(a) *mean solution* (b) *variance of solution*

Figure 7: Comparison of mean and variance of solution for number of samples from stochastic domain.

2. *Stochastic Projection (Normal Distribution)*

The stochastic states $u(t,y)$ $\dot{u}(t,y)$ and $\ddot{u}(t,y)$are computed using the semi-intrusive projection method described in Section A. The mean temporal solution field is obtained as

$$\mathbb{E}[u(t,y)] = u_1(t). \tag{34}$$

The variance is computed as

$$\mathbb{V}[u(t,y)] = \sum_{i=2}^{N} {u_i}^2(t). \tag{35}$$

We use projection method described above for parameter values $\mu_\lambda = 0$ and $\sigma_\lambda = 1$. Figure 8 show comparison of mean and variance computed using projection method with analytical moments for increasing number of terms in spectral expansion. Figure 9 shows the rate of convergence of mean and variance to analytical solutions.

3. *Verification of Random Modes (Normal, Uniform and Exponential)*

Here, we solve the same problem with three choice of distributions: (i) Normal $\mathcal{N}(\mu = 0.0, \sigma = 1.0)$, (ii) Uniform $\mathcal{U}(a = -1.0, b = 1.0)$ and (iii) Exponential $\mathcal{E}(\mu = 0.0, \beta = 1.0)$. The solution is obtained using a stochastic space

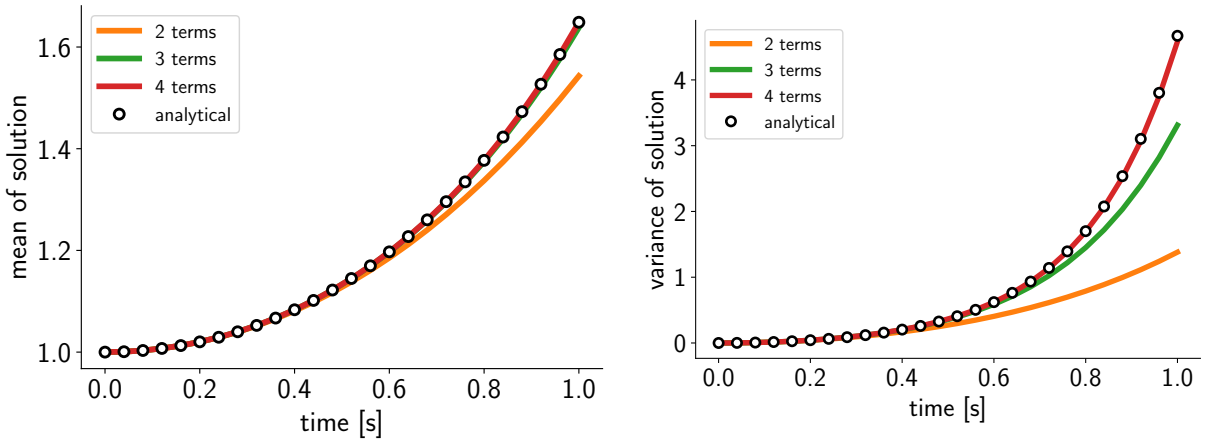

(a) *mean solution* (b) *variance of solution*

Figure 8: Comparison of mean and variance of solution for selected number of terms in polynomial expansion.

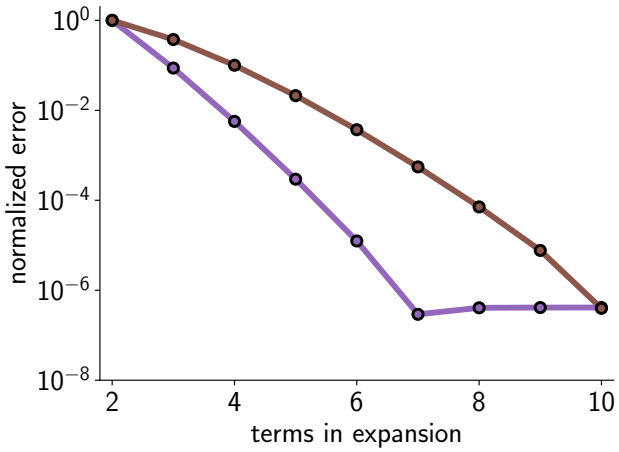

Figure 9: Error convergence of mean (purple) and variance (brown) for number of terms in the orthonormal basis set.

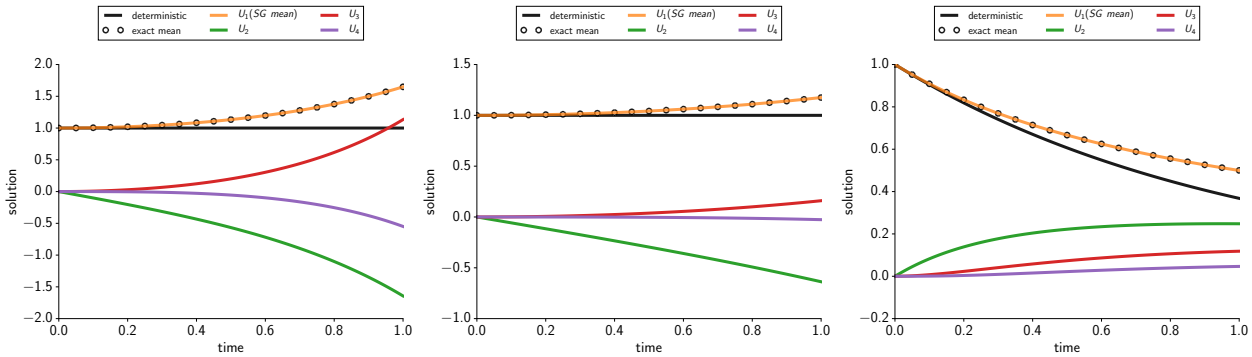

(a) $\mathcal{N}(\mu = 0.0, \sigma = 1.0)$ (b) $\mathcal{U}(a = -1.0, b = 1.0)$ (c) $\mathcal{E}(\mu = 0.0, \beta = 1.0)$

Figure 10: Random modes computed using stochastic Galerkin method along with analytical mean and deterministic solutions for different distribution types.

spanned by $N = 4$ terms, without explicit formation of stochastic equations using the semi-intrusive method described in Section III. Figure 10 plots the solution of the stochastic ODE and all four modes computed, along with deterministic and analytical mean solutions from [9]. It can be seen that the mean of the solution is different than the deterministic

solution in the absence of uncertainties. The mean solution computed using SGM is matching with the analytical solution available to this simple benchmark problem reported in Xiu [9].

B. Pitching and Plunging Airfoil System

We study a second order differential equation in two variables: pitch and plunge variables of an airfoil. This extends the stochastic analysis to vector valued differential equations. We consider the following second-order differential equation with prescribed initial conditions $\vec{u}_0$, $\dot{\vec{u}}_0$ and constant system parameters $[M]$, $[C]$ and $[K]$ in matrix form

$$\begin{aligned} \begin{bmatrix} m & s \\ s & I_f \end{bmatrix} \begin{Bmatrix} \ddot{u}_1(t) \\ \ddot{u}_2(t) \end{Bmatrix} + \begin{bmatrix} c_h & 0 \\ 0 & c_a \end{bmatrix} \begin{Bmatrix} \dot{u}_1(t) \\ \dot{u}_2(t) \end{Bmatrix} + \begin{bmatrix} k_h & 0 \\ 0 & k_a \end{bmatrix} \begin{Bmatrix} u_1(t) \\ u_2(t) \end{Bmatrix} = \begin{Bmatrix} 0 \\ 0 \end{Bmatrix} \quad &\in \quad \mathcal{T} \\ \vec{u}(0) = \vec{u}_0 \quad &\in \quad \partial\mathcal{T} \\ \dot{\vec{u}}(0) = \dot{\vec{u}}_0 \quad &\in \quad \partial\mathcal{T} \end{aligned} \tag{36}$$

The deterministic parameters of the system are listed in Table 2. Let us assume that the mass $m := m(y)$, where y is a

Table 2: Parameters defining the pitching and plunging airfoil system.

Parameter	Definition	Value	Unit
x_f	position of flexural axis	0.25	m
x_{cm}	position of center of mass	0.375	m
m	mass of airfoil	55.3291	kg
I_f	mass moment of inertia of the airfoil around the elastic axis	3.4581	$kg.m^2$
s	static unbalance $m(x_{cm} - x_f)$	6.9161375	$kg.m$
c_h	plunge damping	0	$N/kg/s$
c_a	pitch torsional damping	0	$N.m/kg/s$
k_h	plunge stiffness	11366.0	N/kg
k_a	pitch torsional stiffness	7002.6	$N.m/kg$

random variable from stochastic domain $\mathcal{Y}$. This adds a stochastic dimension to the differential equation resulting in the stochastic differential equation. In $\mathcal{T} \otimes \mathcal{Y}$ we have the vector-valued ordinary differential equation

$$\begin{bmatrix} m(y) & s(y) \\ s(y) & I_f \end{bmatrix} \begin{Bmatrix} \ddot{u}_1(t,y) \\ \ddot{u}_2(t,y) \end{Bmatrix} + \begin{bmatrix} c_h & 0 \\ 0 & c_a \end{bmatrix} \begin{Bmatrix} \dot{u}_1(t,y) \\ \dot{u}_2(t,y) \end{Bmatrix} + \begin{bmatrix} k_h & 0 \\ 0 & k_a \end{bmatrix} \begin{Bmatrix} u_1(t,y) \\ u_2(t,y) \end{Bmatrix} = \begin{Bmatrix} 0 \\ 0 \end{Bmatrix} \tag{37}$$

In $\partial\mathcal{T} \otimes \mathcal{Y}$ we have initial conditions defined as

$$\begin{aligned} \vec{u}(0,y) &= \vec{u}_0 \\ \dot{\vec{u}}(0,y) &= \dot{\vec{u}}_0. \end{aligned} \tag{38}$$

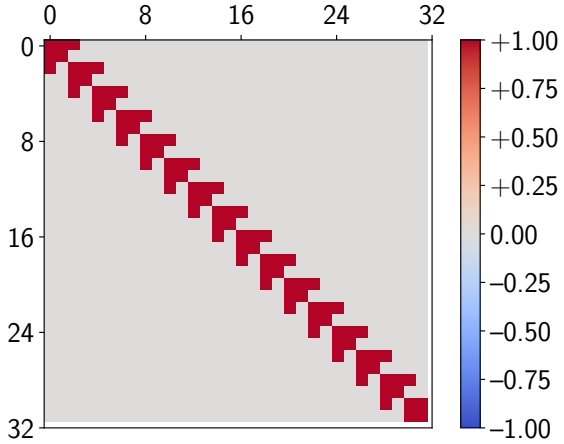

Figure 11: Nonzero pattern of PPA system with one random variable decomposed on a stochastic basis with 16 terms.

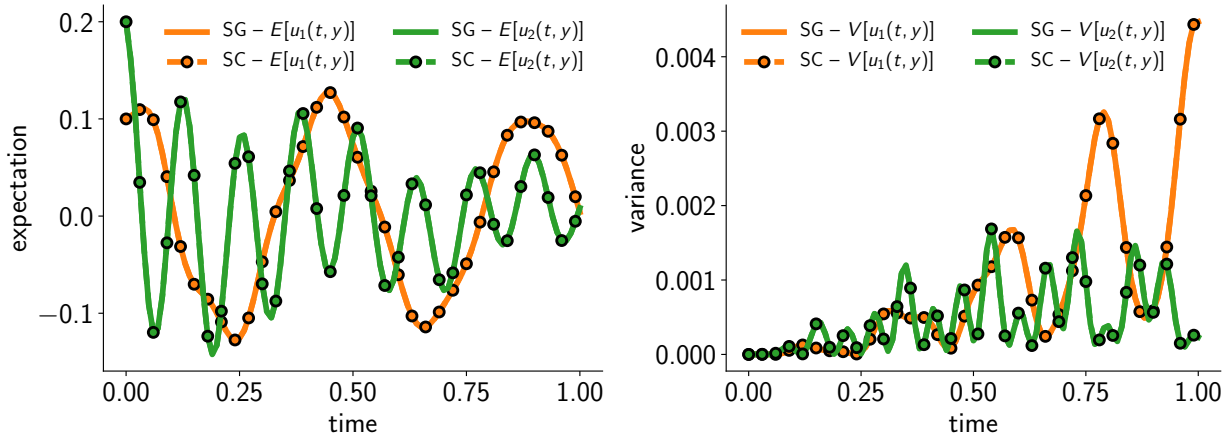

Figure 12: Expectation (left) and variance (right) of solution of pitching-plunging airfoil system obtained using stochastic Galerkin with 5 terms in the basis set and collocation methods with 15 samples.

When using the projection method, an extended linear system is formed. The sparsity of corresponding the stochastic Jacobian for pitching-plungind airfoil system can be visualized from Figure 11. We find the moments of the solution using SGM and SCM and compare them in Figure 12. It can be observed that both the methods are in excellent agreement for both the degrees of freedom (pitch and plunge) and both statistical moments (mean and variance).

C. Spring Mass Damper

We consider the following second-order differential equation with prescribed initial conditions u_0, $\dot{u}_0$ and constant system parameters m, c and k

$$\begin{aligned} m\frac{d^2u(t)}{dt^2} + c\frac{du(t)}{dt} + ku(t) = 0 \quad &\in \quad \mathcal{T} \\ u(0) = u_0 \quad &\in \quad \partial\mathcal{T} \\ \dot{u}(0) = \dot{u}_0 \quad &\in \quad \partial\mathcal{T} \end{aligned} \tag{39}$$

Let us assume that the mass $m := m(y_1)$, damping constant $c := c(y_2)$ and stiffness constant $k := k(y_3)$ where y_1, y_2 and y_3 are independent random variables from three-dimensional stochastic domain $\mathcal{Y}^3$. This dependence on random variables results in stochastic differential equation

$$\begin{aligned} m(y_1)\frac{d^2u(t,\vec{y})}{dt^2} + c(y_2)\frac{du(t,\vec{y})}{dt} + k(y_3)u(t,\vec{y}) = 0 \quad &\in \quad \mathcal{T}\otimes\mathcal{Y}^3 \\ u(0,\vec{y}) = u_0 \quad &\in \quad \partial\mathcal{T}\otimes\mathcal{Y}^3 \\ \dot{u}(0,\vec{y}) = \dot{u}_0 \quad &\in \quad \partial\mathcal{T}\otimes\mathcal{Y}^3 \end{aligned} \tag{40}$$

where $\vec{y} = [y_1, y_2, y_3] \in \mathcal{Y}^3$ is a vector-valued random variable from stochastic space. Let the random variables be $y_1 \sim \mathcal{E}(\mu = 4.0, \beta = 1.0)$, $y_2 \sim \mathcal{U}(a = 0.25, b = 0.75)$, $y_3 \sim \mathcal{N}(\mu = 5.0, \sigma = 0.5)$, and the initial conditions be $u_0 = -0.5$ and $\dot{u}_0 = 1$. The orthonormal space for projection is constructed using tensor product with $N_1 = 4$, $N_2 = 4$ and $N_3 = 4$ functions in each variable, giving rise to 125 terms in the basis. The sparsity pattern arising due to this setup is shown in Figure 13. The mean and variance of the solution field is computed using sampling and projection methods are plotted in Figure 14. The SGM computations were performed using deterministic implementation of the SMD system and the system is solved for time interval of $[0, 10]s$ with a step size of $0.1s$ using BDF2 method. The stochastic collocation (sampling) solutions are computed using a tensor product grid of $15 \times 15 \times 15$. It can be seen that both the solutions are in good agreement with each other.

FUNCTION AND GRADIENT VERIFICATION: The damping coefficient c is chosen to be normally distributed as $\mathcal{N}(\mu = 0.2, \sigma = 0.1)$, and the mass m is treated as the design variable. We are interested in computing the probabilistic moments of the time integral of potential energy

$$F = \int_0^T \frac{1}{2} ku(t)^2 \, dt \tag{41}$$

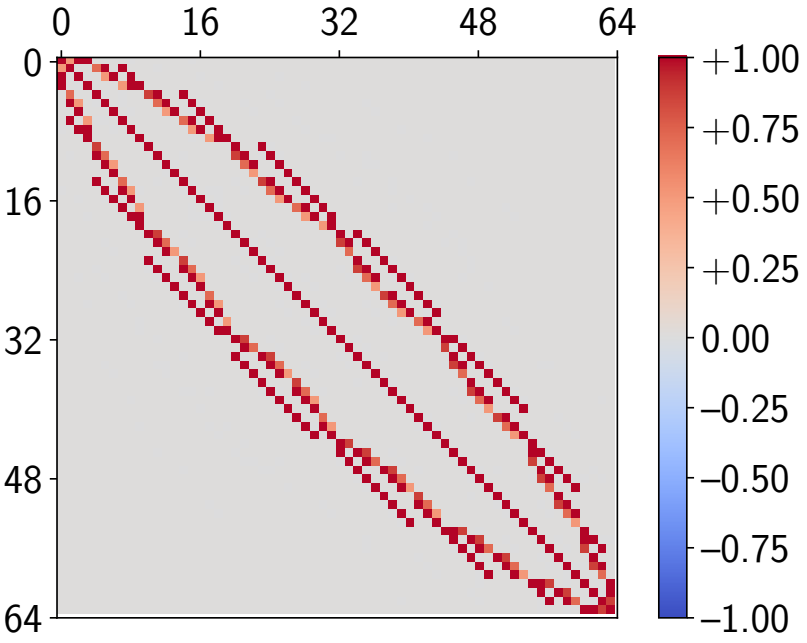

Figure 13: Nonzero pattern of SMD system with 3 random variables y_1, y_2 and y_3 with $N_1 = N_2 = N_3 = 4$ giving rise to 64 basis terms with tensor product.

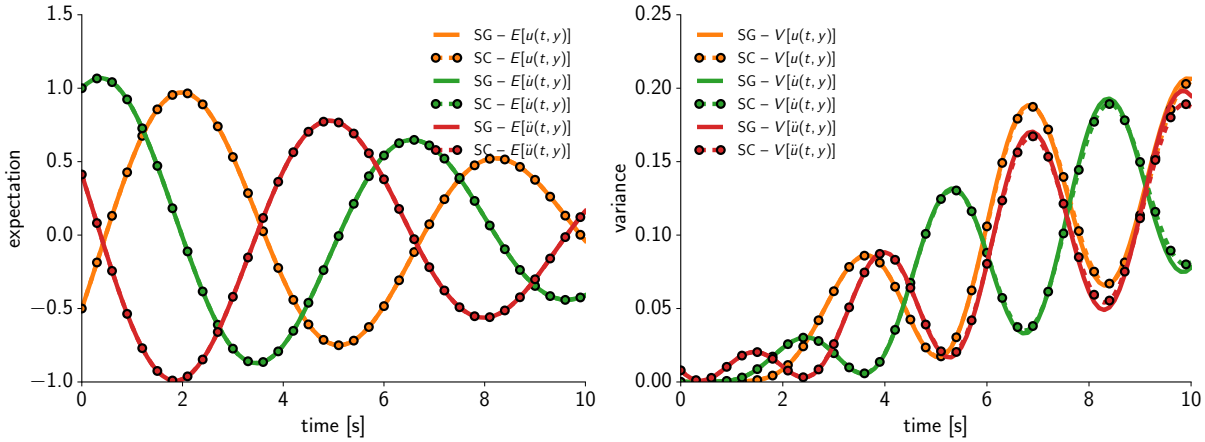

Figure 14: Expectation (top) and variance (bottom) of solution and its time derivatives obtained stochastic collocation and Galerkin methods.

and the Kreisselmeier—-Steinhauser (KS) [59, 60] estimate of the maximum potential energy

$$F = a + \frac{1}{\rho_{ks}} \ln \left[\int_0^T e^{\rho_{ks}\left(\frac{1}{2}ku(t)^2 - a\right)} \, dt \right]. \tag{42}$$

where a and ρ_{ks} are aggregation parameters. The probabilistic moments of (41) and (42) and their design variable derivatives computed using sampling and projection methods are listed in Tables 3 and 4, respectively. It be seen that the stochastic adjoint derivatives exhibit an accuracy of 12 to 15 significant digits.

Table 3: Probabilistic moments and derivatives of the integral of potential energy with 10 basis terms and 10 quadrature samples.

Quantity	Sampling	Projection
$\mathbb{E}[F]$	8.62347899840529308	8.62347899840532683
$\mathbb{V}[F]$	2.18825865715865575	2.18825865715922419
Adjoint $d\mathbb{E}[F]/dm$	2.29637589213232607	2.29637589213362459
Complex-step $d\mathbb{E}[F]/dm$	2.29637589213285809	2.29637589213298554
Error	5.3×10^{-13}	6.4×10^{-13}
Adjoint $d\mathbb{V}[F]/dm$	0.4168637865**27159164**	0.4168637865**19840573**
Complex-step $d\mathbb{V}[F]/dm$	0.4168637865**29946490**	0.4168637865**28287372**
Error	2.8×10^{-12}	8.4×10^{-12}

Table 4: Probabilistic moments and derivatives of the maximum potential energy in time domain with 10 basis terms and 10 quadrature samples.

Quantity	Sampling	Projection
$\mathbb{E}[F]$	2.502**93127981364005**	2.507**08458655184918**
$\mathbb{V}[F]$	3.8**12548135154223 78** $\times 10^{-3}$	3.8**01475524796593 67** $\times 10^{-3}$
Adjoint $d\mathbb{E}[F]/dm$	-3.69267283814**737500** $\times 10^{-3}$	-3.69267283814**618151** $\times 10^{-3}$
Complex-step $d\mathbb{E}[F]/dm$	-3.69267283815**061589** $\times 10^{-3}$	-3.69267283815**030625** $\times 10^{-3}$
Error	3.2×10^{-15}	2.5×10^{-14}
Adjoint $d\mathbb{V}[F]/dm$	-8.594229333**69482361** $\times 10^{-3}$	-8.594229333**68299627** $\times 10^{-3}$
Complex-step $d\mathbb{V}[F]/dm$	-8.594229333**70226558** $\times 10^{-3}$	-8.594229333**70156128** $\times 10^{-3}$
Error	7.4×10^{-15}	8.1×10^{-14}

D. Four Bar Mechanism

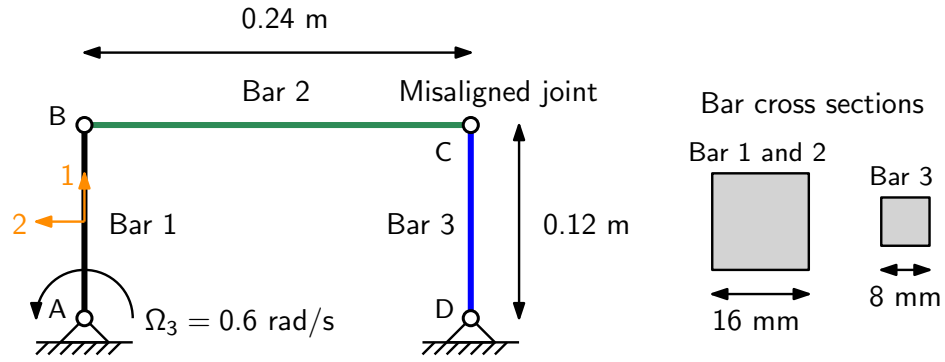

Figure 15: The four-bar mechanism problem.

As a final example, we show the application of the proposed semi-intrusive projection technique to the four bar mechanism benchmark [61]. Figure 15 illustrates the setup of the four bar mechanism. The problem contains three bars that are modeled using Timoshenko beam elements, three revolute joints and an actuator driving the mechanism. An imaginary, infinitely rigid fourth bar exists in the mechanism between the points A and D. The revolute joints at points A, B, and D, and have an axis of rotation that is perpendicular to the plane of the mechanism. However, the revolute joint at point C is misaligned by an angle of 5°, and rotated about the direction of the bar CD. This misalignment angle is subject to uncertainty and distributed normally with $\mathcal{N}(\mu = 5°, \sigma = 2.5°)$. Bars AB and BC are of the same cross-section, while bar CD has a smaller cross section. The rotation of bar AB about point A of the mechanism is driven at an angular rate of $\Omega_3 = 0.6$ rad/s.

The finite element library TACS is used for deterministic, stochastic sampling and stochastic projection based solution of the four bar mechanism problem. In the stochastic projection case, the black-box finite element analysis code TACS is extended in a modular fashion to compute the probabilistic moments of quantities of interest and their derivatives.

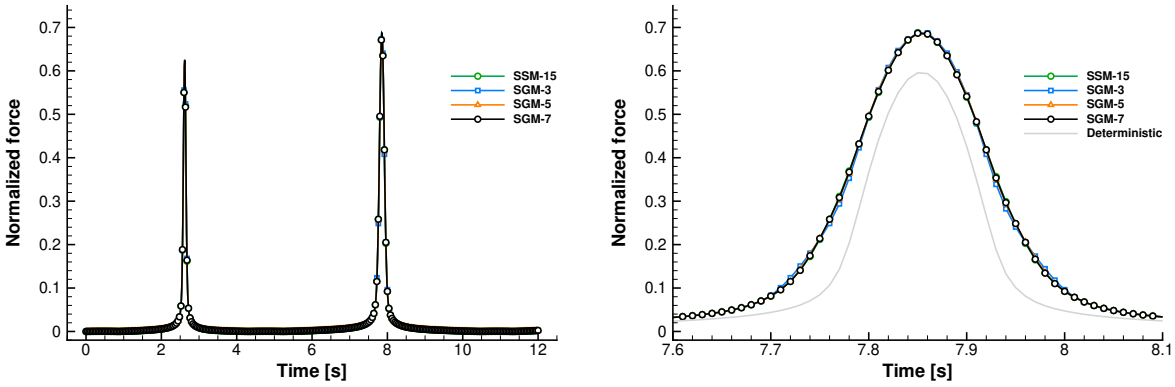

Figure 16: The mean of normalized axial force in bar AB as a function of time predicted using SGM and SSM.

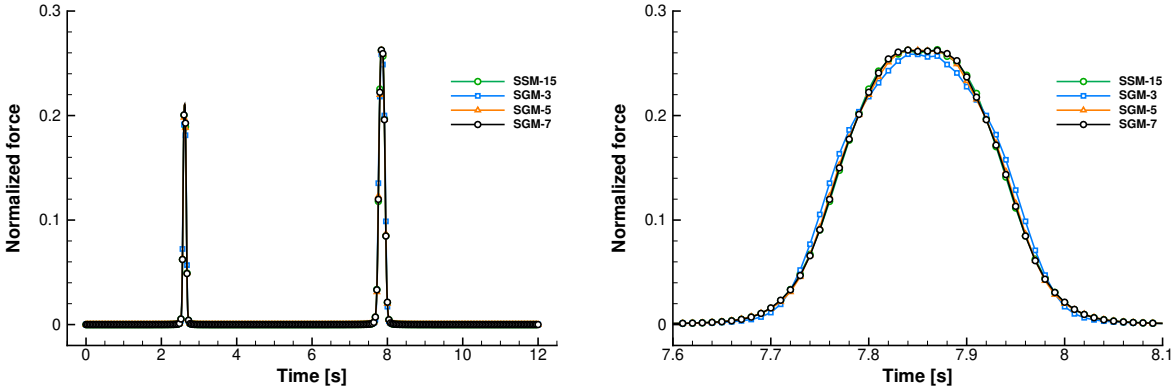

Figure 17: The variance of the normalized axial force in bar AB as a function of time predicted using SGM and SSM.

Figure 16 shows the behavior of the mean of the normal force in the bar AB computed using SGM with 3, 5, and 7 terms in the spectral basis compared with SSM using 15 sample point locations. Overall, the normal force exhibits two large peaks that occur as the mechanism is forced to snap through the angle where it would lock if the bars were rigid due to the misaligned joint. The overall behavior of the mean axial force is shown in Figure 16 as well as a zoomed in view of the behavior between $t = 7.6$ and $t = 8.1$ which centers on the second large spike in axial force. SGM captures the peak behavior in the normal force, even with only three terms. Note that the deterministic solution under-predicts the mean maximum force.

Figure 17 shows the variance of the axial force in the bar AB computed using SGM with 3, 5, and 7 terms in the spectral basis compared with SSM using 15 sample point locations. Again, the distribution of the variance exhibits two large peaks. The second zoomed in view of the variance illustrates that SGM again captures the overall behavior with only 3 terms. However, better agreement is obtained between SSM and SGM as more SGM basis functions are added.

V. Conclusions

The stochastic Galerkin projection method offers an efficient approach to propagate uncertainties through complex, nonlinear simulations. However, challenges can arise when implementing SGM and the adjoint method for OUU. In this paper, we demonstrated a framework for SGM based on the deterministic finite-element code TACS. This framework leverages existing deterministic element implementations to provide the terms needed for analysis

and adjoint-based gradient evaluation. The main idea of the proposed semi-intrusive technique is to project the deterministic element residuals, Jacobians, boundary conditions, and adjoint terms on to the probabilistic space prior to assembly of the stochastic finite element system, assuming the deterministic implementations to be black-box. The mean and variance of the implemented SGM were compared to the mean and variance computed using sampling methods to demonstrate the accuracy of SGM. The accuracy of the adjoint method was verified using complex-step methods. Future work will consider the application of the proposed framework to OUU problems.

References

[1] R. Ghanem and P. D. Spanos. *Stochastic Finite Elements: A Spectral Approach (2nd edition)*. New York: Springer, 1991.

[2] H. G. Matthies. *Uncertainty Quantification with Stochastic Finite Elements*, chapter 27. John Wiley & Sons, 2007. ISBN 9780470091357. doi:10.1002/0470091355.ecm071. URL https://onlinelibrary.wiley.com/doi/abs/10.1002/0470091355.ecm071.

[3] M. A. Gutirrez and S. Krenk. *Stochastic Finite Element Methods*, chapter 20. John Wiley & Sons, 2004. ISBN 9780470091357. doi:10.1002/0470091355.ecm044. URL https://onlinelibrary.wiley.com/doi/abs/10.1002/0470091355.ecm044.

[4] D. Xiu. *Numerical Methods for Stochastic Computations: A Spectral Method Approach*. Princeton University Press, 2010. ISBN 978-0691142128.

[5] O. P. L. Maître and O. M. Knio. *Spectral Methods for Uncertainty Quantification, Scientific Computation*. Springer, 2010. ISBN 978-9048135196.

[6] R. Ghanem, H. Owhadi, and D. Higdon. *Handbook of uncertainty quantification*. 06 2017. doi:10.1007/978-3-319-12385-1.

[7] C. Soize. *Uncertainty Quantification*, volume 47. 01 2017. doi:10.1007/978-3-319-54339-0.

[8] M. Gunzburger. *An Applied/Computational Mathematicians View of Uncertainty Quantification for Complex Systems: Proceedings of 2015 and 2016 ACMES Conferences*, pages 133–151. 01 2019. ISBN 978-1-4939-9050-4. doi:10.1007/978-1-4939-9051-1_5.

[9] D. Xiu. Fast Numerical Methods for Stochastic Computations: A Review. *Comm. Comput. Phys.*, 5, No. 2–4:242–272, 2009.

[10] A. Keane and P. Nair. *Computational Approaches for Aerospace Design*. John Wiley & Sons, 2005.

[11] K. Boopathy and M. P. Rumpfkeil. *Robust Optimizations of Structural and Aerodynamic Designs*. doi:10.2514/6.2014-2595. URL https://arc.aiaa.org/doi/abs/10.2514/6.2014-2595.

[12] K. Boopathy, M. P. Rumpfkeil, and R. M. Kolonay. *Robust Optimization of a Wing Under Structural and Material Uncertainties*. doi:10.2514/6.2015-0920. URL https://arc.aiaa.org/doi/abs/10.2514/6.2015-0920.

[13] S. Hosder, R. W. Walters, and R. Perez. A non-intrusive polynomial chaos method for uncertainty propagation in CFD simulations. AIAA Paper, 2006-891, 2006.

[14] M. S. Elred, C. G. Webster, and P. G. Constantine. Evaluation of Non-Intrusive Approaches for Wiener-Askey Generalized Polynomial Chaos. AIAA Paper, 2008-1892, 2008.

[15] B. A. Jones, A. Doostan, and G. H. Born. Nonlinear Propagation of Orbit Uncertainty Using Non-Intrusive Polynomial Chaos. *AIAA Journal of Guidance, Control, and Dynamics*, 36, No.2:415–425, 2013.

[16] G. Fishman. *Monte-Carlo: Concepts, Algorithms, and Applications*. New York: Springer-Verlag, 1996.

[17] B. Peherstorfer, M. Gunzburger, and K. Willcox. Convergence analysis of multifidelity Monte Carlo estimation. *Numerische Mathematik*, 139:1–25, 01 2018. doi:10.1007/s00211-018-0945-7.

[18] M. S. Elred. Recent Advances in Non-Intrusive Polynomial Chaos and Stochastic Collocation Methods for Uncertainty Analysis and Design. AIAA Paper, 2009-2274, 2009.

[19] H. Cheng and A. Sandu. Collocation least-squares polynomial chaos method. SCS/ACM, 2010.

[20] M. Gunzburger, C. G. Webster, and G. Zhang. *Sparse Collocation Methods for Stochastic Interpolation and Quadrature*, pages 717–762. 06 2017. doi:10.1007/978-3-319-12385-1_29.

[21] O. Roderick, M. Anitescu, and P. Fischer. Polynomial Regression Approaches Using Derivative Information for Uncertainty Quantification. *J. of Nuclear Science and Engineering*, 164, No.2:122–139, 2010.

[22] Y. Li, M. Anitescu, O. Roderick, and F. Hickernell. Orthogonal Bases for Polynomial Regression with Derivative Information in Uncertainty Quantification. *International Journal for Uncertainty Quantification*, 1, No.4:297–320, 2011.

[23] M. P. Rumpfkeil. Optimizations Under Uncertainty Using Gradients, Hessians, and Surrogate Models. *AIAA Journal*, 51, No. 2:444–451, 2013.

[24] M. P. Rumpfkeil. Robust design under mixed aleatory/epistemic uncertainties using gradients and surrogates. *Journal of Uncertainty Analysis and Applications*, 1(1):7, Oct 2013. ISSN 2195-5468. doi:10.1186/2195-5468-1-7. URL https://doi.org/10.1186/2195-5468-1-7.

[25] T. Chatterjee, R. Chowdhury, and P. Ramu. Decoupling uncertainty quantification from robust design optimization. *Structural and Multidisciplinary Optimization*, 59(6):1969–1990, Jun 2019. ISSN 1615-1488. doi:10.1007/s00158-018-2167-0. URL https://doi.org/10.1007/s00158-018-2167-0.

[26] O. Ernst and E. Ullmann. Stochastic Galerkin Matrices. *SIAM Journal on Matrix Analysis and Applications*, 31(4):1848–1872, 2010. doi:10.1137/080742282. URL https://doi.org/10.1137/080742282.

[27] P. Delgado and V. Kumar. A stochastic Galerkin approach to uncertainty quantification in poroelastic media. *Applied Mathematics and Computation*, 266:328–338, 2015. ISSN 0096-3003. doi:https://doi.org/10.1016/j.amc.2015.04.127. URL http://www.sciencedirect.com/science/article/pii/S0096300315006001.

[28] D. Xiu and G. E. Karniadakis. The Wiener-Askey Polynomial Chaos for Stochastic Differential Equations. *SIAM Journal of Scientific Computing*, 24(2):619–644, 2002.

[29] R. Ghanem and J. Red-Horse. Propagation of Probabilistic Uncertainty in Complex Physical Systems Using a Stochastic Finite Element Approach. *Physica D*, 133:137–144, 1999.

[30] R. Ghanem. Ingredients for a general purpose stochastic finite elements implementation. *Computer Methods in Applied Mechanics and Engineering*, 168(1):19 – 34, 1999. ISSN 0045-7825. doi:https://doi.org/10.1016/S0045-7825(98)00106-6. URL http://www.sciencedirect.com/science/article/pii/S0045782598001066.

[31] M. D. Gunzburger, C. G. Webster, and G. Zhang. Stochastic finite element methods for partial differential equations with random input data. *Acta Numerica*, 23:521–650, 05 2014. doi:10.1017/S0962492914000075.

[32] R. Abgrall and S. Tokareva. The Stochastic Finite Volume Method. *SEMA SIMAI Springer Series*, pages 1–57, 01 2017. doi:10.1007/978-3-319-67110-9_1.

[33] G. Taguchi. *Quality Engineering through Design Optimization*. Kraus International Publications, New York, 1984.

[34] G. Taguchi. *Introduction to Quality Engineering*. American Supplier Institute, 1989.

[35] P. Kouvelis and G. Yu. *Robust Discrete Optimization and Its Applications*. Kluwer, 1997.

[36] A. Ben-Tal, L. E. Ghaoui, and A. Nemirovski. *Robust Optimization*. Princeton Series in Applied Mathematics, Princeton University Press, 2009.

[37] S. Sundaresan, K. Ishii, and D. R. Houser. A ROBUST OPTIMIZATION PROCEDURE WITH VARIATIONS ON DESIGN VARIABLES AND CONSTRAINTS. *Engineering Optimization*, 24(2):101–117, 1995. doi:10.1080/03052159508941185. URL https://doi.org/10.1080/03052159508941185.

[38] M. M. Putko, A. C. Taylor III, P. A. Newmann, and L. L. Green. Approach for Input Uncertainty Propagation and Robust Design in CFD Using Sensitivity Derivatives. *Journal of Fluids Engineering*, 124(1):60–69, 2002.

[39] C. R. Gumbert, P. A. Newman, and G. J. Hou. Effect of random geometric uncertainty on the computational design of 3-D wing. AIAA Paper, 2002-2806, June, 2002.

[40] Y. Cao, M. Y. Hussaini, and T. A. Zang. An efficient Monte Carlo method for optimal control problems with uncertainty. *Computational Optimization and Applications*, 26(3):219–230, 2003.

[41] J. M. Luckring, M. J. Hemsch, and J. H. Morrison. Uncertainty in computational aerodynamics. AIAA Paper, 2003-0409, January, 2003.

[42] Y. Cao, M. Y. Hussaini, T. A. Zang, and A. Zatezalo. A variance reduction method based on sensitivity derivatives. *Applied Numerical Mathematics*, 56:800–813, 2006.

[43] A. Ben-Tal, L. E. Ghaoui, and A. Nemirovski. Foreword: special issue on robust optimization. *Mathematical Programming*, 107(1-2):1–3, 2006.

[44] F. Chalot, Q. Dinh, E. Herbin, L. Martin, M. Ravachol, and G. Roge. Estimation of the impact of geometrical uncertainties on aerodynamic coefficients using CFD. AIAA Paper, 2068-2008, April, 2008.

[45] W. Chen, J. Allen, K. Tsui, and F. Mistree. Procedure for Robust Design: Minimizing Variations Caused by Noise Factors and Control Factors. *Journal of Mechanical Design*, 118(4):478–485, 1996.

[46] W. Chen and X. Du. Towards a Better Understanding of Modeling Feasibility Robustness in Engineering Design. *Journal of Mechanical Design*, 122(4):385–394, 1999.

[47] K. Zaman, M. McDonald, S. Mahadevan, and L. Green. Robustness-based Design Optimization Under Data Uncertainty. *Structural and Multidisciplinary Optimization*, pages 1–15, 2011.

[48] Z. Mourelatos and J. Liang. A Methodology for Trading-off Performance and Robustness Under Uncertainty. *Journal of Mechanical Design*, 128:856, 2006.

[49] G. Park, T. Lee, H. Kwon, and K. Hwang. Robust Design: an Overview. *AIAA Journal*, 44(1):181–191, 2006.

[50] X. Du and W. Chen. Methodology for Managing the Effect of Uncertainty in Simulation-Based Design. *AIAA Journal*, 38(8): 1471–1478, 2000.

[51] D. Padmanabhan, H. Agarwal, J. Renaud, and S. Batill. A study using Monte Carlo Simulation for failure probability calculation in Reliability-Based Optimization. *Optimization and Engineering*, 7(3):297–316, 2006. ISSN 1389-4420. doi:10.1007/s11081-006-9973-8.

[52] R. Paiva, A. Carvalho, C. Crawford, A. Suleman, and R. Canfield. A Robust and Reliability-Based Design Optimization Framework for Wing Design. AIAA Paper, 2010-2919, 2010.

[53] H. Agarwal. *Reliability Based Design Optimization: Formulations and Methodologies*. PhD thesis, University of Notre Dame, 2004.

[54] A. Parkinson, C. Sorensen, and N. Pourhassan. A general approach for robust optimal design. *Trans. ASME*, 115:74–80, 1993.

[55] X. Du and W. Chen. Towards a better understanding of mod-eling feasibility robustness in engineering design. *ASME Journal of Mechanical Design*, 122(4):385–394, 2000.

[56] S. Rangavajhala, A. Mullur, and A. Messac. The challenge of equality constraints in robust design optimization: examination and new approach. *Structural and Multidisciplinary Optimization*, 34(5):381–401, Nov 2007. ISSN 1615-1488. doi:10.1007/s00158-007-0104-8. URL https://doi.org/10.1007/s00158-007-0104-8.

[57] K. Boopathy and G. J. Kennedy. Parallel Finite Element Framework for Rotorcraft Multibody Dynamics and Discrete Adjoint Sensitivities. *AIAA Journal*, 0(0):1–14, 2019. doi:10.2514/1.J056585. URL https://doi.org/10.2514/1.J056585.

[58] K. Boopathy and G. Kennedy. Adjoint-based derivative evaluation methods for flexible multibody systems with rotorcraft applications. In *55th AIAA Aerospace Sciences Meeting*, Grapevine, TX, January 2017. doi:10.2514/6.2017-1671.

[59] G. Kreisselmeier and R. Steinhauser. Systematic control design by optimizing a vector performance index. In *International Federation of Active Controls Symposium on Computer-Aided Design of Control Systems*, Zurich, Switzerland, 1979.

[60] G. J. Kennedy and J. E. Hicken. Improved constraint-aggregation methods. *Computer Methods in Applied Mechanics and Engineering*, 289:332 – 354, 2015. ISSN 0045-7825. doi:10.1016/j.cma.2015.02.017.

[61] O. A. Bauchau, P. Betsch, A. Cardona, J. Gerstmayr, B. Jonker, P. Masarati, and V. Sonneville. Validation of flexible multibody dynamics beam formulations using benchmark problems. *Multibody System Dynamics*, 37(1):29–48, may 2016. ISSN 1573-272X. doi:10.1007/s11044-016-9514-y. URL https://doi.org/10.1007/s11044-016-9514-y.